Available online: journal.ipb.ac.id/index.php/jphpi


# CHARACTERIZATION OF EARTHQUAKE-RESISTANT CONCRETE PROPERTIES INCORPORATING BARNACLE'S $CaCO_3$ NANOPARTICLES AND *BACILLARIOPHYCEAE*'S BIOSILICA

**Esa Ghanim Fadhallah[1]*, Resti Sabilla[1], Annisa Yasmine Aulia[1], Affandi Prayoga[1], Zaky Adrian[2], Afrido Rahmanda[2], Eka Herlina Fatimatuzzahro[2], Azka Kautsar Lustrilanang[1], Zaskia Rahma Andini[1], Zidane Aulia Rivai[1]**
[1]Department of Agricultural Product Technology, Faculty of Agriculture, University of Lampung
Prof. Dr. Ir. Sumantri Brojonegoro st. No.1, Bandar Lampung, Lampung Indonesia 35141
[2]Department of Civil Engineering, Faculty of Engineering, University of Lampung
Prof. Dr. Ir. Sumantri Brojonegoro st. No.1, Bandar Lampung, Lampung Indonesia 35141

Submitted: 23 October 2025/Accepted: 2 April 2026
*Correspondence: esa.ghanim@fp.unila.ac.id

**How to cite (APA Style 7th):** Fadhallah, E. G., Sabilla, R., Aulia, A. Y., Prayoga, A., Adrian, Z., Rahmanda, A., Fatimatuzzahro, E. H., Lustrilanang, A. K., Andini, Z. R., & Rivai, Z. A. (2026). Characterization of earthquake-resistant concrete properties incorporating barnacle's $CaCO_3$ nanoparticles and *Bacillariophyceae's* biosilica. *Jurnal Pengolahan Hasil Perikanan Indonesia,* 29(7), 596-607. http://dx.doi.org/10.17844/vdzvpf19

## Abstract

The megathrust phenomenon along the southern coast of Java Island highlights the need for earthquake-resistant and sustainable construction material. Designing earthquake-resilient structures requires concrete mixtures that can dampen seismic vibrations while maintaining cost efficiency. This study aimed to determine the optimum incorporation level of barnacle-derived $CaCO_3$ nanoparticles and *Bacillariophyceae* as cement-substitution additives in earthquake-resistant concrete. The additives were incorporated at substitution levels of 0% (control), 5%, 10%, 15%, 20%, and 25%of cement using a fixed $CaCO_3$:biosilica ratio of 1:1 (w/w). The characterization of materials included X-ray Fluorescence (XRF), Fourier-transform infrared (FTIR), and Particle Size Analysis (PSA) for $CaCO_3$ nanoparticles, while biosilica was characterized using XRF. The concrete performance was evaluated through compressive and flexural strength using a Compression Testing Machine (CTM) and Universal Testing Machine (UTM) at 14 and 28 days. XRF analysis showed that barnacle shells contained 91.72% Ca, whereas biosilica contained 98.79% $SiO_2$. The synthesized $CaCO_3$ nanoparticles had an average particle size of 120.1 nm. Mechanical testing revealed that the optimal substitution level (5%) resulted in a 16% reduction in compressive strength and a 4.6% reduction in flexural strength compared to the control, achieving maximum compressive and flexural strengths of 21.26 MPa and 4.10 MPa, respectively. Substitution within the range of 5-10% provides the best balance between strength and material efficiency in earthquake-resistant concrete formulations. These findings suggest that barnacle-derived $CaCO_3$ and Bacillariophyceae biosilica can serve as sustainable cement substitutes for eco-efficient and earthquake-resistant construction materials in coastal regions.

Keywords: cement substitution, compressive strength, flexural strength, marine biowaste, seismic

http://dx.doi.org/10.17844/vdzvpf19

# Karakterisasi Beton Tahan Gempa dari Nanopartikel $CaCO_3$ Teritip dan Biosilika *Bacillariophyceae*

**Abstrak**

Isu megatumbukan di selatan Pulau Jawa menegaskan perlunya pengembangan material konstruksi yang tahan gempa dan berkelanjutan. Perancangan konstruksi tahan gempa membutuhkan campurann beton yang mampu meredam getaran seismik dengan tetap mempertahankan efisiensi biaya. Penelitian ini bertujuan menentukan tingkat penambahan optimum nanopartikel $CaCO_3$ dari teritip dan biosilika dari *Bacillariophyceae* sebagai bahan substitusi sebagian semen pada beton tahan gempa. Konsentrasi bahan substitusi meliputi 0% (kontrol), 5%, 10%, 15%, 20%, dan 25% dari berat semen dengan rasio tetap $CaCO_3$:biosilika sebesar 1:1 (b/b). Karakterisasi material meliputi *X-Ray Fluorescence* (XRF), *Fourier Transform Infrared* (FTIR), dan *Particle Size Analysis* (PSA) untuk nanopartikel $CaCO_3$, sedangkan biosilika dikarakterisasi menggunakan XRF. Kinerja beton dievaluasi melalui pengujian kuat tekan dan kuat lentur menggunakan *Compression Testing Machine* (CTM) dan *Universal Testing Machine* (UTM) pada umur 14 dan 28 hari. Hasil analisis XRF menunjukkan bahwa cangkang teritip mengandung 91,72% Ca, sedangkan biosilika mengandung 98,79% $SiO_2$. Nanopartikel $CaCO_3$ yang dihasilkan memiliki ukuran partikel rata-rata 120,1 nm. Pengujian mekanis menunjukkan bahwa tingkat substitusi optimum sebesar 5% menghasilkan penurunan kuat tekan sebesar 16% dan kuat lentur 4,6% dibandingkan kontrol, dengan nilai maksimum masing-masing 21,26 Mpa dan 4,10 MPa. Hasil penelitian ini menunjukkan bahwa substitusi 5-10% memberikan keseimbangan terbaik antara kekuatan dan efisiensi bahan dalam formulasi beton tahan gempa. $CaCO_3$ dari teritip dan biosilika *Bacillariophyceae* berpotensi dimanfaatkan sebagai substituen semen yang berkelanjutan untuk menghasilkan material konstruksi tahan gempa yang ramah lingkungan dan efisien, khususnya di wilayah pesisir.

Kata kunci: substitusi semen, kuat lentur, kuat tekan, seismik, limbah laut

## INTRODUCTION

Indonesia is one of the countries with the highest geological disaster vulnerability. The World Risk Report (2024) records Indonesia as the second most disaster-prone nation globally, with a risk index score of 41.13 on a scale of 100. This high level of vulnerability is closely linked to Indonesia's geological setting, which lies at the convergence of four major tectonic plates: the Eurasian, Indo-Australian, Pacific, and Philippine plates. The interaction of these plates forms complex subduction zones that generate geodynamic activities, such as subduction, plate displacement, and the formation of faults and volcanic arcs, all of which can trigger large-scale earthquakes and tsunamis (Hutchings and Mooney, 2021). This places Indonesia, particularly the southern region of Java Island, among the areas with the highest seismic risk in the Indo-Pacific region (Pribadi *et al*., 2023).

Historically, major seismic activity in Java, especially in West Java, has exhibited a periodic pattern, indicating the potential for recurring events. Historical records show that this region experienced two megathrust earthquakes with magnitudes exceeding 7.5 in 1903 and 1921, and another with a magnitude exceeding 7.8 in 2006 (Supendi *et al*., 2022). These findings suggest that megathrust earthquakes in this region have an approximate return period of 100 yr. Furthermore, tsunami modeling conducted by Widiyantoro *et al*. (2020) revealed that in a worst-case scenario, if two megathrust segments rupture simultaneously, tsunami wave heights could reach 12–20 m, with an average maximum height of approximately 4.5 m along the southern coast of Java. This evidence underscores that the southern coastal region of Java faces a genuine threat of major earthquakes and tsunamis, with the potential for severe structural damage, loss of life, and substantial economic losses. Therefore, response to this threat, the development of building materials that are resistant to seismic loads has become an important priority in disaster mitigation efforts.

Resilient infrastructure protects communities during disasters and ensures long-term economic efficiency. The construction sector contributes approximately 10 percent to Indonesia's GDP as of 2022, with concrete being the dominant material across various development sectors. Investment in earthquake-resistant buildings has proven to be cost-effective in the long term, with construction costs being only approximately 5 percent higher than those of conventional buildings, but significantly reducing repair and reconstruction expenses (Mirani *et al.*, 2024). According to SNI 2847:2019 (BSN, 2019), concrete is defined as a homogeneous mixture of cement, aggregate, and water, with a maximum compressive strength of 35 MPa for special structural frames and wall systems. Aljaafreh *et al.* (2023) emphasized that earthquake-resistant concrete is designed to possess ductility and the ability to absorb and dissipate seismic energy through controlled plastic deformation. This mechanism prevents sudden collapse, allowing the structure to remain standing for a longer time and providing sufficient evacuation time (Arifin and Jonrinaldi, 2024). Ideal earthquake-resistant concrete should employ a mix capable of vibration damping while remaining cost-efficient, which can be achieved through the incorporation of $CaCO_3$ derived from barnacles (*Balanus* sp.) as a value-added additive.

Barnacles (*Balanus* sp.) are marine invertebrates that inhabit intertidal and subtidal zones, with an average density of 45 individuals per square meter in coral reef habitats (Wibawa *et al.*, 2022). Their shells are composed of approximately 90–95 percent $CaCO_3$, which can be converted into precipitated calcium carbonate (PCC) or nano-PCC (particle size below 0.1 μm). These materials have been shown to increase the tensile strength of concrete by up to 25 percent and function as effective structural binders (Paramitha *et al.*, 2023). Because of their non-pozzolanic nature, barnacle-derived $CaCO_3$ requires nanoscale modification to enable reactions with calcium hydroxide and promote pozzolanic reactions that enhance mechanical properties and reduce concrete permeability (Al-Lezami and Devi, 2022; Suparmi *et al.* 2021).

In addition to $CaCO_3$, biogenic silica derived from microalgae of the class *Bacillariophyceae* (diatoms) holds great potential as an eco-friendly concrete additive. These phytoplankton are widely distributed in tropical waters, with more than 100,000 known species that grow optimally at silica concentrations above 0.5 mg/L (Malviya *et al.*, 2016; Haque *et al.*, 2024). Their cell walls contain abundant amorphous silica that reacts with calcium hydroxide to form additional binding compounds, thereby strengthening the concrete matrix. Moreover, their porous microstructure improves absorption and reduces permeability by up to 15 percent, thereby enhancing compressive strength and crack resistance (Arman *et al.*, 2024; Paramitasari *et al.*, 2024). The incorporation of diatomite has also been reported to improve the physical and mechanical properties of concrete while reducing its fluidity, which is critical for maintaining structural stability under dynamic loading conditions (Li *et al.*, 2023).

Previous studies have explored the use of marine biominerals to improve the performance of concrete (Suryawanshi & Shaikh, 2021; Wang *et al.*, 2024; Jasni *et al.*, 2024). However, no specific investigation has addressed the potential of barnacle-derived $CaCO_3$ nanoparticles combined with diatom biosilica as a cement substitute. This study examined how these two biominerals might address the inherent brittleness of conventional concrete. Nano-$CaCO_3$ from barnacles can reinforce the internal structure by filling microscopic voids, whereas biosilica from diatoms is expected to improve vibration absorption. This combination is intended to create a more resilient matrix that can better withstand intense shaking and reduce the risk of sudden structural failure. Therefore, this study aimed to determine the optimum incorporation level of barnacle-derived $CaCO_3$ nanoparticles and *Bacillariophyceae* biosilica as cement-substitution additives in earthquake-resistant concrete. This

http://dx.doi.org/10.17844/vdzvpf19

approach is expected to provide an innovative and sustainable solution for mitigating megathrust earthquake risks while optimizing the utilization of locally available marine resources.

## MATERIALS AND METHOD

### Isolation of Biosilica

The isolation of biosilica from diatoms followed the modified sol-gel method described by Utama *et al.* (2025). Diatomaceous earth was purchased from a certified supplier. A total of 20 g of diatomaceous earth was weighed using an analytical balance (KERN ABS 220-4) and homogenized in 500 mL of 1 M NaOH solution at 60–80°C for 3 h. The resulting suspension was titrated with 1 M HCl at 60–80°C and allowed to stand overnight to form a silica hydrogel. The hydrogel was washed with distilled water and oven-dried to produce biosilica in powder form.

### Preparation of $CaCO_3$ Nanoparticles from Barnacles

Barnacle shells were collected in July 2025 from coastal structures in Teluk Kunyit and from the shorelines of Sariringgung and Mutun, all located within Lampung Province, Indonesia. The samples were then cleaned, sun-dried, and ground using a grinder at the Agricultural Product Processing Laboratory. The preparation procedure was based on the method of Prihanto *et al.* (2022) to obtain $CaCO_3$ powder using the dry milling method. A total of 100 g of $CaCO_3$ barnacle shell powder was placed in a ball mill (MYRA-YFI56) together with 16 steel balls with a diameter of 2 cm, and run at a speed of 200 rpm for 70 h. The milled powder was then sieved and dried at a low temperature (<80°C) to obtain stable nano-sized particles without any changes in the $CaCO_3$ phase. The samples were analyzed for particle size using a particle size analyzer (Beckman Coulter) to confirm the nanoscale range. Element characterization was performed using XRF (PANalytical, model Minipal 4) to identify calcium (Ca) and FTIR to detect $CO_3$ functional groups (Hariyati *et al.*, 2019).

### Concrete Mix Design

The concrete job mix formula (JMF) was designed to achieve a target compressive strength of 25 MPa at 28 days. The formulation followed the SNI 7656:2012 (BSN, 2012) mix design method and was conducted at the Materials and Construction Laboratory of the University of Lampung. Additives of $CaCO_3$ from barnacles (*Balanus* sp.) and *Bacillariophyceae* biosilica in a 1:1 ratio were incorporated at substitution levels of 0, 5, 10, 15, 20, and 25% relative to the cement weight. This range was used to evaluate a broad performance spectrum, from low-dosage enhancement to higher substitution levels, and to identify the specific threshold where the bio-additives transition from improving the matrix to potentially reducing compressive strength. The process began with formulation calculations, aggregate weighing, and mixing using a concrete mixer (TIGER GT300 GE). The resulting mixture was subjected to a slump test, and each variation was cast into three cylindrical molds (15 cm diameter × 30 cm height) and three beam molds (15 × 15 × 60 cm). After compaction using a vibrator and plastic covering, the concrete was cured before testing on days 14 and 28. The concrete formulation is presented in Table 1.

### Compressive Strength Test

Compressive strength tests were performed using a CTM (Vertex Scientific) in accordance with SNI 1974:2011 (BSN, 2011) at the Materials and Construction Laboratory. The samples were positioned with a maximum plate spacing of 1 cm, and the indicator needle was reset to zero before loading at a rate of 0.15–0.35 MPa/s until the maximum load (Pmax, in kN) was reached. The test results are presented as mean ± standard deviation to reflect sample variability.

### Flexural Strength Test

Flexural strength tests were conducted following SNI 4431:2011 (BSN, 2011) using a UTM (Zwick Roell) at the Materials and Construction Laboratory. Once the specimen was properly positioned, the load was gradually applied at a rate of 8–10 kg/cm² per

Table 1 Concrete mix design with varying levels of cement substitution using barnacle-derived $CaCO_3$ and biosilica

| Substitution level (%) | Coarse aggregate (kg) | Fine aggregate (kg) | Water (kg) | Cement (kg) | $CaCO_3$(kg) | Biosilica (kg) |
|---|---|---|---|---|---|---|
| 0 | 24.1859 | 17.1166 | 3.6026 | 9.2640 | 0 | 0 |
| 5 | 24.1859 | 17.1166 | 3.6026 | 8.8008 | 0.2316 | 0.2316 |
| 10 | 24.1859 | 17.1166 | 3.6026 | 8.3376 | 0.4632 | 0.4632 |
| 15 | 24.1859 | 17.1166 | 3.6026 | 7.8744 | 0.6948 | 0.6948 |
| 20 | 24.1859 | 17.1166 | 3.6026 | 7.4112 | 0.9264 | 0.9264 |
| 25 | 24.1859 | 17.1166 | 3.6026 | 6.9480 | 1.1580 | 1.1580 |

minute to prevent sudden impact and then reduced near the cracking point. The peak load causing failure was recorded at three measurement points with a precision of 0.25 mm, and the average value was calculated.

## Data Analysis

Data were analyzed descriptively, including silica (Si) and calcium (Ca) detection using X-ray fluorescence (XRF) (with normalized data), and compound identification of $CaCO_3$ using Fourier-transform infrared spectroscopy (FTIR) and particle size analysis (PSA). The mechanical properties of the concrete were determined based on the maximum values recorded from the UTM and CTM tests and further statistically analyzed using IBM SPSS version 25.

## RESULTS AND DISCUSSION

### Analysis of XRF and FTIR

Characterization of biosilica derived from *Bacillariophyceae* diatoms using X-Ray Fluorescence (XRF) analysis revealed a $SiO_2$ content of 98.798% (Table 2), indicating high purity and excellent potential as a supplementary material for concrete. The characterization of barnacle-derived $CaCO_3$ showed a calcium content of 91.72% (Table 2). The Fourier transform infrared (FTIR) spectrum of barnacle $CaCO_3$ (Figure 1) exhibited characteristic vibrational bands corresponding to C–H stretching at 2519.7 cm$^{-1}$, O–H stretching between 3750 and 3000 cm$^{-1}$, and C–O stretching within the 1300–1000 cm$^{-1}$ range. In addition, carbonate ion ($CO_3^{2-}$) vibrations were detected between 716.6–1796.6 cm$^{-1}$ (Vironika & Rahmawati,

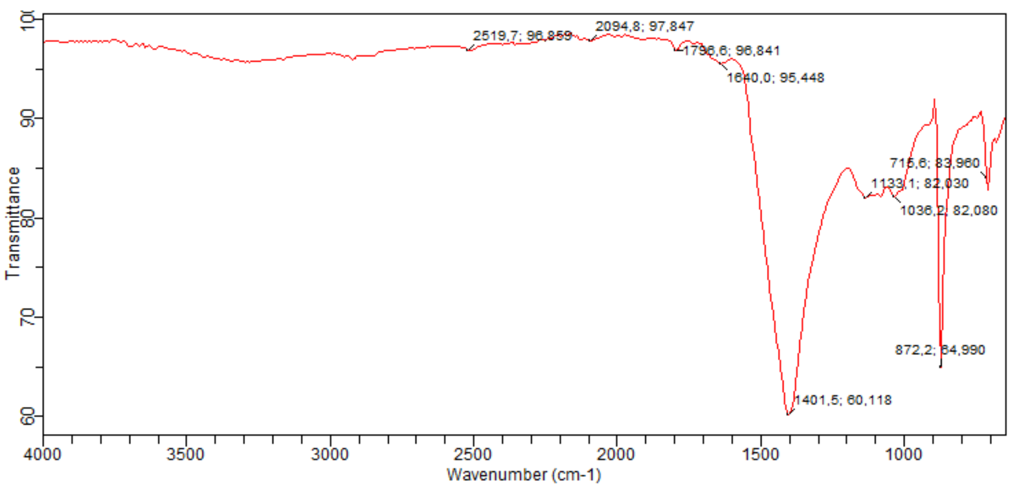


Figure 1 FTIR spectra of nanoparticle $CaCO_3$ from barnacle shell

Table 2 Elemental composition of barnacle shells and diatoms

| Element | Sample | | Compound | Sample | |
|---|---|---|---|---|---|
| | Barnacle shell (%) | Diatom (%) | | Barnacle shell (%) | Diatom (%) |
| Na | 2.186 | 0.000 | $Na_2O$ | 2.557 | 0.000 |
| Mg | 0.282 | 0.000 | MgO | 0.400 | 0.000 |
| Al | 0.048 | 0.296 | $Al_2O_3$ | 0.077 | 0.335 |
| Si | 0.975 | 97.553 | $SiO_2$ | 1.775 | 98.798 |
| P | 0.005 | 0.016 | $P_2O_5$ | 0.010 | 0.011 |
| S | 0.800 | 0.000 | $SO_3$ | 1.622 | 0.000 |
| Cl | 1.601 | 0.029 | Cl | 1.269 | 0.009 |
| K | 0.252 | 0.162 | $K_2O$ | 0.231 | 0.057 |
| Ca | 91.715 | 0.467 | CaO | 90.331 | 0.189 |
| Ti | 0.069 | 0.124 | $TiO_2$ | 0.074 | 0.059 |
| V | 0.005 | 0.053 | $V_2O_5$ | 0.006 | 0.027 |
| Cr | 0.002 | 0.006 | $Cr_2O_3$ | 0.001 | 0.003 |
| Mn | 0.066 | 0.004 | MnO | 0.055 | 0.001 |
| Fe | 0.618 | 1.243 | $Fe_2O_3$ | 0.569 | 0.496 |
| Ni | 0.002 | 0.002 | NiO | 0.002 | 0.001 |
| Cu | 0.028 | 0.004 | CuO | 0.023 | 0.001 |
| Zn | 0.014 | 0.026 | ZnO | 0.012 | 0.009 |
| As | 0.001 | 0.001 | $As_2O_3$ | 0.000 | 0.000 |
| Sr | 1.200 | 0.005 | SrO | 0.909 | 0.001 |
| Y | - | 0.001 | $Y_2O_3$ | - | 0.000 |
| Zr | 0.009 | 0.003 | $ZrO_2$ | 0.008 | 0.001 |
| Sb | 0.006 | 0.001 | CdO | 0.000 | 0.000 |
| Te | 0.014 | - | $Sb_2O_3$ | 0.004 | 0.000 |
| Ba | 0.019 | 0.003 | BaO | 0.014 | 0.001 |
| Hg | 0.000 | 0.000 | HgO | 0.000 | 0.000 |
| Pb | 0.001 | 0.000 | PbO | 0.001 | 0.000 |

2022). A distinct absorption peak at 872.2 $cm^{-1}$ (Riyanto *et al.*, 2023) indicates the presence of calcium oxide (CaO), confirming that $CaCO_3$ was successfully identified in the synthesized barnacle nanoparticles.

## Particle Size Analysis

Particle size analysis of barnacle-derived $CaCO_3$ revealed that all particles were within the nanometer range, distributed between 10 and 201.5 nm, with an average of 120.1 nm (Figure 2). This confirms that the synthesized material meets the nanoparticle size criteria proposed by Eker *et al.* (2024), who defined nanoparticles as having dimensions of up to 100 nm in at least one spatial direction (x, y, or z). The small particle size and large specific surface area significantly influence interparticle interactions and enhance the pozzolanic reactivity of $CaCO_3$. According

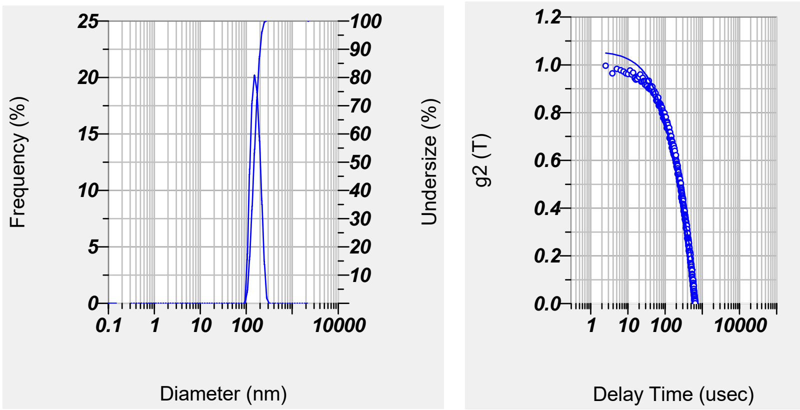


Figure 2 Particle size distribution of barnacle-derived $CaCO_3$ nanoparticles

to Mydin *et al.* (2023), incorporating nanoparticles into concrete can improve its workability, mechanical strength, durability, and microstructural properties. Barnacle-derived $CaCO_3$ nanoparticles act as nucleation sites for the formation of calcium silicate hydrate (C–S–H) gel, which forms through reactions between calcium hydroxide and silicate compounds present in the cement matrix. This mechanism contributes to enhanced bonding within the matrix and leads to improved compressive strength of concrete.

## Compressive Strength

The compressive strength of concrete with $CaCO_3$ nanoparticles and biosilica is presented in Table 3.

The compressive strength test results showed that the strength of the concrete increased with the curing age. This finding is consistent with the statement of Marchewka *et al.* (2025), who explained that a longer curing period allows the cement hydration process to proceed more completely, leading to the formation of more calcium silicate hydrate (C–S–H) compounds that significantly contribute to concrete strength development. Optimal curing conditions, such as temperature, humidity, and time control, ensure that hydration reactions occur efficiently, minimizing the risk of early cracking and promoting a notable increase in strength at later ages. Therefore, the experimental data obtained are in agreement with the theoretical principle that the compressive strength of concrete is directly proportional to the curing duration.

Table 3 indicates that the addition of $CaCO_3$ nanoparticles and biosilica influenced the mechanical performance of concrete at different curing ages ($p$<0.05). The control sample (0% substitution) exhibited the highest compressive strength, reaching 24.28 MPa at 14 d and 25.33 MPa at 28 d. This indicates

Table 3 Compressive strength (MPa) of concrete from $CaCO_3$ nanoparticle and biosilica

| Substitution (%) | Day 14 | Day 28 |
|---|---|---|
| 0 | $24.28\pm0.39^{a}$ | $25.33\pm0.46^{a}$ |
| 5 | $13.47\pm0.66^{b}$ | $21.26\pm0.37^{b}$ |
| 10 | $12.20\pm0.28^{b}$ | $20.09\pm0.12^{b}$ |
| 15 | $9.19\pm0.27^{c}$ | $17.11\pm0.16^{c}$ |
| 20 | $8.23\pm0.32^{c}$ | $16.18\pm0.25^{c}$ |
| 25 | $6.46\pm0.65^{d}$ | $12.49\pm0.69^{d}$ |

Values followed by different superscript letters within the same column are significantly different according to Duncan's Multiple Range Test at a 95% confidence level ($p$<0.05)

http://dx.doi.org/10.17844/vdzvpf19

that a conventional concrete composition without substitution still provides optimal bonding and hydration reactions under standard curing conditions. However, the incorporation of $CaCO_3$ nanoparticles and biosilica led to varying effects, depending on the substitution level. At 5% substitution, the compressive strength at 28 d increased to 21.26 MPa, indicating a moderate improvement compared to the 14-day strength. This suggests that small additions of nanoparticles can contribute to secondary hydration and enhance microstructural densification during curing. Nano-$CaCO_3$ provides nucleation sites for calcium silicate hydrate (C–S–H) formation, while biosilica reacts with calcium hydroxide to form additional C–S–H, both of which strengthen the matrix. These findings are consistent with those of Suryawanshi and Shaikh (2021), who reported a 6.9% improvement in compressive strength when *Meretrix casta* shell powder was used at a 5% substitution level. Similarly, Rahmadani *et al.* (2025) demonstrated that 7% substitution of *Anadara granosa* shell powder achieved a compressive strength of 28.16 MPa at 28 d, indicating that shell-based materials tend to exhibit optimal compressive performance at low to moderate substitution levels.

Beyond the 10% substitution level, a decline in compressive strength was observed, with values decreasing progressively to 17.11 MPa at 15%, 16.18 MPa at 20%, and 12.49 MPa at 25% substitution, on day 28. This reduction may be attributed to the excessive replacement of cement, which limits the availability of calcium hydroxide necessary for pozzolanic reactions and disrupts the matrix continuity. Dhairiyasamy *et al.* (2025) explained that nanomaterials start to clump together rather than spread evenly at higher concentrations. These clumps or agglomerates create internal weak spots and tiny voids in concrete. From a durability perspective, these extra pores are problematic because they can increase water absorption, which eventually weakens the structure. In a major earthquake, these microscopic gaps act as 'stress points' where the concrete can start to crush under the heavy vertical pressure of a building (El-Feky *et al.*, 2024), making the 10% limit a critical threshold for maintaining the structural safety.

Similar findings were reported by Al-Lezami and Devi (2022), who noted that high nanoparticle loading can cause particle agglomeration, reducing the packing efficiency and overall strength. Overall, the compressive strength data exhibited a parabolic trend, improving at low substitution levels (up to 5%) before declining as the percentage increased. This trend reflects the balance between the beneficial microstructural refinement at optimal nanoparticle concentrations and the detrimental effects of excessive substitution. Microstructurally, nano-$CaCO_3$ and biosilica enhanced the particle packing density and filled the capillary pores, potentially improving the interfacial bonding between the aggregates and cement matrix. Although the compressive strength decreased beyond 10% substitution, this microstructural uniformity may enhance the ductility and energy absorption capacity of the material under cyclic loading, which are crucial properties for earthquake-resistant concrete.

## Flexural Strength

The flexural strength of concrete with $CaCO_3$ nanoparticles and biosilica is presented in Table 4.

The flexural strength results of concrete with varying levels of $CaCO_3$ nanoparticles and biosilica substitution are presented in Table 4. Overall, the data indicate that the flexural strength of all mixtures increased with curing age, consistent with the findings of Jin *et al.* (2025), who reported that prolonged curing enhances cement hydration and leads to a denser microstructural bond within the concrete matrix. This densification improves the material's ability to resist tensile strength and crack propagation, resulting in higher flexural strength values at later ages.

At 14 days, the control sample (0% substitution) exhibited the highest flexural strength (3.27 MPa), whereas increasing substitution levels resulted in a gradual decrease in strength. However, by day 28, a significant strength gain was observed across all formulations, indicating that the hydration and pozzolanic reactions of the supplementary materials continued to

Table 4 Flexural strength (MPa) of concrete from $CaCO_3$ nanoparticle and biosilica

| Substitution (%) | Day 14 | Day 28 |
|---|---|---|
| 0 | 3.27±0.37[a] | 4.30±0.42[a] |
| 5 | 2.28±0.40[b] | 4.10±0.14[a] |
| 10 | 2.23±0.32[b] | 4.06±0.08[a] |
| 15 | 1.46±0.64[c] | 3.27±0.38[b] |
| 20 | 1.43±0.60[c] | 3.11±0.15[b] |
| 25 | 1.39±0.55[c] | 2.37±0.52[c] |

Values followed by different superscript letters within the same column are significantly different according to Duncan's Multiple Range Test at a 95% confidence level ($p<0.05$)

progress over time. The 5% substitution level achieved a flexural strength of 4.10 MPa at 28 days, approaching that of the control (4.30 MPa), suggesting an optimal balance between the filler and binder phases at this concentration. Similarly, Suryawanshi and Shaikh (2021) reported a modest flexural strength increase of approximately 3.9% with the addition of *Meretrix casta* shell powder at a 5% substitution level. In contrast, at higher substitution levels (≥20%), the flexural strength declined significantly ($p<0.05$), likely due to the dilution effect and reduced calcium hydroxide availability, which limits secondary C–S–H formation. This phenomenon weakens the interfacial bonding and increases the porosity, as reported by Al-Lezami and Devi (2022). From a microstructural perspective, moderate nanoparticle incorporation improves the packing density and refines the pore structure, enhancing load transfer and crack-bridging capacity under bending stress.

These results suggest that the moderate incorporation of $CaCO_3$ nanoparticles and biosilica can contribute positively to the flexural performance of concrete, particularly when sufficient curing time is provided to ensure full hydration and pozzolanic reactivity. However, excessive substitution may hinder matrix cohesion, resulting in reduced flexural capacity. The observed trends align well with the established hydration mechanisms and the theory that longer curing durations enhance the development of interfacial bonding and load transfer efficiency within the cementitious composite. Furthermore, the improvement in flexural strength observed at low substitution levels indicates enhanced ductility and energy absorption capacity, which are key characteristics of earthquake-resistant concrete. The refined microstructure formed by the addition of nano-$CaCO_3$ and biosilica not only strengthened the matrix but also increased its ability to dissipate energy and delay crack propagation under cyclic loading, thereby improving the overall seismic resilience of the structure.

## CONCLUSIONS

This study demonstrated that barnacle-derived $CaCO_3$ nanoparticles and *Bacillariophyceae* biosilica can be utilized as partial cement substitutes for earthquake-resistant concrete. The optimum substitution level was 5%, resulting in compressive and flexural strengths of 21.26 MPa and 4.10 MPa at 28 days, respectively. Substitution levels of 5-10% provided the most favorable balance between mechanical performance and material efficiency. Therefore, these marine-derived biomaterials show potential as sustainable alternatives for reducing cement consumption in earthquake-resistant-concrete applications. Future studies should explore the long-term durability of these composites in seismic environments. In addition, testing under dynamic loading is necessary to better simulate actual earthquake vibrations and confirm the reliability of the material for structural applications.

## ACKNOWLEDGMENT

The authors would like to express their sincere gratitude to the Director General of Research and Development, Ministry of Higher Education, Science, and Technology, for funding support under Decree number 279/C/C2/KPT/2025, awarded to Esa Ghanim Fadhallah.

## REFERENCES

Aljaafreh, A., Alzubi, Y., Al-Kharabsheh, E., & Yasin, B. (2023). Seismic performance of reinforced concrete structures with concrete deficiency caused by in-situ quality management issues. *Civil Engineering Journal*, 9(8), 1957–1970.

Al-Lezami, H. A., & Devi, G. (2022). Synthesis of calcium carbonate nanoparticles and its application in grey water treatment. *IOP Conference Series: Earth and Environmental Science*, 1055(1), 1–7.

Arifin, A. S. R., & Jonrinaldi. (2024). Cost estimation analysis of construction projects on simple earthquake-resistant houses. *Journal of Civil Engineering and Vocational Education*, 11(1), 13–19.

Arman, A., Nugroho, F., Mulyati, & Azman, H. F. (2024). Pengaruh penambahan silika fume terhadap kuat tekan beton. *Jurnal Teknologi dan Vokasi*, 2(1), 9–16.

[BSN] Badan Standardisasi Nasional. (2011). *SNI 1974:2011 Cara Uji Kuat Tekan Beton dengan Benda Uji Silinder*. Badan Standardisasi Nasional.

[BSN] Badan Standardisasi Nasional. (2011). *SNI 4431:2011 Cara Uji Kuat Lentur Beton Normal dengan Dua Titik Pembebanan*. Badan Standardisasi Nasional.

[BSN] Badan Standardisasi Nasional. (2012). *SNI 7656:2012 Tata Cara Pemilihan Campuran untuk Beton Normal, Beton Massa*. Badan Standardisasi Nasional.

[BSN] Badan Standardisasi Nasional. (2019). *SNI 2847:2019 Persyaratan Beton Struktural untuk Bangunan Gedung dan Penjelasan*. Badan Standardisasi Nasional.

Dhairiyasamy, R., Gabiriel, D., Varshney, D., & Singh, S. (2025). Optimizing nanomaterial dosages in concrete for structural applications using experimental design techniques. *Scientific Reports*, 15(1), 22375.

Eker, F., Duman, H., Akdasci, E., Bolat, E., Saritas, S., Karav, S., & Witkowska, A. M. (2024). A comprehensive review of nanoparticles: from classification to application and toxicity. *Molecules*, 29(15), 1–83.

El-Feky, M. S., Badawy, A. H., & Helal, Y. H. (2024). Nanotechnology-enabled innovations in cement: enhancing durability, and impact load resistance with nanocellulose, nano silica, and nano clay additives. *Egyptian Journals of Chemistry*, 68(7), 223-231.

Haque, M. Z., Afiati, N., & Jati, O. E. (2024). Kadar silika ($SiO_2$) terhadap kelimpahan diatom bentik di Sungai Jamblang Kabupaten Cirebon. *Bioscientist*, 12(1), 14–27.

Hariyati, Shofiyani, A., & Wibowo, M. A. (2019). Ekstraksi kalsium karbonat ($CaCO_3$) dari bahan dasar cangkang kerang ale-ale (*Meretrix meretrix*) pada temperatur kalsinasi 500°C. *Jurnal Kimia Khatulistiwa*, 8(1), 54–58.

Henry, D. P., & McLaughlin, P. A. (1975). The barnacles of the *Balanus amphitrite* complex (Cirripedia, Thoracica). *Zoologische Verhandelingen*, 141(1), 1–254.

Hutchings, S. J., & Mooney, W. D. (2021). The seismicity of Indonesia and tectonic implications. *Geochemistry, Geophysics, Geosystems*, 1–42.

Jasni, S. A., Muthusamy, K., Ruslan, H. N., Hamada, H. M., & Wahab, E. S. A. (2024). Use of seashell as cement replacement in construction material: A review. *Construction*, 4(1), 7–20.

Jin, A. H., Woo, J. S., Yun, H. D., Kim, S. W., Park, W. S., & Choi, W. C. (2025). Influence of concrete strength and fiber properties on residual flexural strength of steel fiber reinforced concrete. *Construction and Building Materials*, 489, 1–19.

Li, C., Li, G., Chen, D., Gao, K., Cao, Y., Zhou, Y., Mao, Y., Fan, S., Tang, L., & Jia, H. (2023). The effects of diatomite as an additive on the macroscopic properties and microstructure of concrete. *Materials*, 16(5), 1–16.

Malviya, S., Scalco, E., Audic, S., Vincent, F., Veluchamy, A., Poulain, J., Wincker, P., Ludicone, D., Vargas, C., Bittner, L., Zingone, A., & Bowler, C. (2016). Insights into global diatom distribution and diversity in the world's ocean. *Proceedings of the National Academy of Sciences*, 113(11), 1–10.

Marchewka, A., Ziolkowski, P., & Galan, S. G. (2025). Real-time prediction of early concrete compressive strength using AI and hydration monitoring. *Scientific Reports*, 15(1), 1–25.

Mirani, Z., Natalia, M., Mafriyal, S., Sari, D., & Hanum, R. F. (2024). Comparison costs of building conventional house and earthquake resistant house concept based on analysis benefit cost ratio of 50 years earthquake scenario. *Jurnal Ilmiah Poli Rekayasa*, 19(2), 76–86.

Mydin, M. Z. O., Jagadesh, P., Bahrami, A., Dulaimi, A., Ozkilic, Y. O., Abdullah, M. M. A. B., & Jaya, R. P. (2023). Use of calcium carbonate nanoparticles in production of nano-engineered foamed concrete. *Journal of Materials Research and Technology*, 26, 4405–4422.

Paramitasari, D., Musa, Putra,O.P., Suparman, Pramana, Y.S.,Sarah, E., Hidayat, T., Thajono, A.E., Meidiawati, D.P., Pudjianto, K., Supriyanti.A. 2024. Hydroxypropylation for functional enhancement of sago starch: The effects of low propylene oxide concentration using response surface methodology. *Journal of Agriculture and Food Research*,15.100933.

Paramitha, L., Pratama, R. A., & Kurniati, E. (2023). Sintesis nano-precipitated calsium carbonate dari cangkang bekicot dengan penambahan polimer PEG 400. *CHEMPRO*, 4(1), 8–14.

Pribadi, K. S., Abduh, M., Wirahadikusumah, R. D., Hanifa, N. R., Irsyam, M., Kusumaningrum, P., & Puri, E. (2021). Learning from past earthquake disasters: The need for knowledge management system to enhance infrastructure resilience in Indonesia. *International Journal of Disaster Risk Reduction*, 64(1), 1–18.

Prihanto, A., Muryanto, S., Ismail, R., Jamari, J., & Bayuseno, A. P. (2022). Utilization of green mussel shell waste for calcium carbonate synthesis through the carbonation method with temperature variation. *IOP Conference Series: Earth and Environmental Science*, 1098(1), 1–7.

Rahmadani, I., Nurmeyliandari, R., & Amalia, G. (2025). Pemanfaatan limbah cangkang kerang dara sebagai substitusi semen terhadap kuat tekan beton. *Jurnal Mira Teknik Sipil*, 8(2), 501-506.

Riyanto, B., Trilaksani, W., & Rahmaeni, N. (2023). Kalsium oksida cangkang kerang sebagai material reaksi eksotermis kemasan pemanas sendiri untuk pangan darurat lokal. *Jurnal Teknologi Perikanan dan Kelautan*, 14(2), 137–147.

Sukma, A. M., & Takarina, N. D. (2022). Relationship of diatom phytoplankton (*Bacillariophyceae*) diversity with water quality and heavy metal in Angke and Grogol Rivers, Jakarta City. *IOP Conference Series: Earth and Environmental Science*, 1083(1), 1–7.

Suparmi, Dewita, Desmelati, Hidayat, T. Study of the making of hydrolizate protein powder of rebon shrimp as a food nutrition enhancement ingredient. *Pharmacognosy Journal,* 13(5):1180-1185.

Supendi, P., Widiyantoro, S., Rawlinson, N., Yatikmantoro, T., Muhari, A., Hanifa, N. R., Gunawan, E., Shiddqi, H. A., Imran, I., Anugrah, S. D., Daryono, D., Prayitno, B. S., Adi, S. P., Kaernawati, D., Faizal, L., & Damanik, R. (2022). On the potential for megathrust earthquakes and tsunamis off the southern coast of West Java and southeast Sumatra, Indonesia. *Natural Hazards*, 116, 1315–1328.

Suryawanshi, V. V., & Shaikh, A. N. (2021). Experimental study on behavior of concrete for replacement of fly ash and sea shells as a substitute to cement and coarse aggregates. *International Journal*

http://dx.doi.org/10.17844/vdzvpf19

*for Scientific Research and Development*, 8(1), 223–229.

Telussa, I., & Rahayu. (2022). Isolation and frustule characterization of diatoms *Navicula* sp. *Tad Strains: Jurnal Biosains Pascasarjana*, 24(2), 76–81.

Utama, M. D., Ariani, N., Machmud, E., Mude, A. H., Dharma, M. A. T., Taqwim, A., & Risnawati, R. (2025). Synthesis and application of sol-gel-derived nano-silica in glass ionomer cement for dental cementation. *Biomimetics*, 10(235), 1–12.

Vironika, A. O., & Rohmawati, L. (2022). Sintesis $CaCO_3$ dari dolomit Bangkalan dengan metode leaching. *Sains dan Matematika*, 7(1), 39–42.

Wang, X., Yu, H., Li, F., Nikolayevich, K. S., Yu, H., Nikolaevich, L. S., & Fan, W. (2024). Effect of biological shells aggregate on the mechanical properties and sustainability of concrete. *Scientific Reports*, 14(1), 1–16.

Wibawa, W. D. P., Ahyadi, H., Hadi, I., & Candri, D. A. (2022). Keanekaragaman teritip pada tiga ekosistem (hutan mangrove, padang lamun, dan terumbu karang) di Perairan Sekotong. *Samota Journal of Biological Sciences*, 1(1), 27–38.

Widiyantoro, S., Gunawan, E., Muhari, A., Rawlinson, N., Mori, J., Hanifa, N. R., Susilo, S., Supendi, P., Shiddiqi, H. A., Nugraha, A. D., & Putra, H. E. (2020). Implications for megathrust earthquakes and tsunamis from seismic gaps south of Java, Indonesia. *Scientific Reports*, 10(15274), 1–12.

*World Risk Report*. (2024). *World Risk Report: Multiple Crises*. World Risk Report Publisher.